

The effect of molecular structure of polypropylene on stretchability for biaxially oriented film

著者	Tamura Satoshi, Kuramoto Itaru, Kanai Toshitaka
journal or publication title	Polymer Engineering and Science
volume	52
number	6
page range	1383-1393
year	2012-06-01
URL	http://hdl.handle.net/2297/32281

doi: 10.1002/pen.22180

The effect of molecular structure of polypropylene on stretchability for biaxially oriented film

Satoshi Tamura, Itaru Kuramoto, Toshitaka Kanai*

Prime Polymer Co., Ltd., Idemitsu Kosan Co., Ltd.*

580-30, Nagaura, Sodegaura-city, Chiba, 299-0265 JAPAN

1-1, Anesaki-Kaigan, Ichihara-city, Chiba, 299-0193 JAPAN*

Abstract

Biaxially oriented polypropylene films are widely used for food packaging and industrial films. Recently machine speed has been increasing in order to obtain higher production rate and film thickness has become thinner to reduce the environmental load. The customers' requirements for better production ability and thinner films have been becoming more demanding, but their demands are not always met due to lack of film stretchability in the final product. In order to meet the demands, research on stretchability has been conducted with the goal of finding the optimum polypropylene molecular structure for developing a new product by analyzing stretching force-strain data using a table tenter which was thought to be the parameter of stretchability. It was found that low crystallinity and wide molecular weight distribution were effective in improving the stretchability from the table tenter test. By running the test with a sequential and biaxially oriented stretching machine, it was verified that samples produced by the above designed polymer indicated good thickness uniformity which was considered to be the barometer of stretchability. Furthermore, it was concluded that analyzing the stretching force-strain data obtained from a table tenter is a good method to predict machine speed and film thickness.

Introduction

About 40 million tons per year of Polypropylene (PP) are currently produced in the world [1]. Biaxially Oriented Polypropylene (BOPP) film accounts for a large amount of PP since it is suited for food packaging films or industrial films, because of its high performance in terms of mechanical and optical properties. Recently higher production speeds are required to reduce the production costs and thinner films are requested for the purpose of reducing the environmental load. Yet there are some cases when PP products do not satisfy the demands due to a lack of stretchability. In those cases, film breaking occurs at transverse direction (TD) stretching process when it is produced by a sequential and biaxially oriented stretching machine (Fig.1). And film quality also drops because of wrinkles created by low thickness uniformity.

To overcome the problem, various studies have been performed by many researchers. For example, the stretchability of various stretching process was studied [2-7] and the relationship between the stress-strain curve of uniaxial stretching and deforming of PP crystal was studied using a spectral birefringence technique by various researchers. However the results did not show any relationship with stretchability [8]. Phillips et al. reported the relationship between stress-strain curve and the crystal structure of biaxially oriented film, but there was no indication of the influence of the stress-strain curve on the stretchability [9].

Kanai gave a report on the prediction of film thickness uniformity using the stress-strain curve in his reports [10, 11]. The relationship between strain (stretching ratio) and stretching force is indicated in Fig.2. In this paper, the stretching process can be divided into three regions in terms of thickness uniformity. Where there's lower stretching ratio at the beginning of stretching (region I), the stretching force increases in proportion to stretching ratio showing local maximum force. At the middle stage (region II), the stretching force indicates the flat line, and at the last stage (region III) the stretching force increases again with increasing stretching ratio [12-14]. Fig.2 also shows the thickness uniformity with the cross-sectional view of film. It is well known that PP is stretched unevenly, which is called neck-like deformation at a lower stretching ratio. From the beginning to the middle stage of stretching, thickness uniformity gradually worsens. At the later stage (region III) thickness uniformity improves because the highly stretched part has a higher stretching force than the lower stretched part, and the lower stretched part becomes easier to stretch with a low stretching force. This has been observed in uniaxial, simultaneous biaxial and sequential biaxial stretching experiments in other resin such as polyethylene terephthalate (PET) [15] and polyetheretherketone (PEEK) [16].

There are some reports regarding the relationship between the stress-strain curve and molecular structure of PP. The stretching force at the yield point was related to the degree of crystallinity as reported by Butler et al. [17], deformation of crystal as reported by Phillips et al. [18], and the thickness of lamella as reported by Kanai et

al. [11, 13]. Consequently, the crystallinity of PP is considered to be the influence factor to the stretching force at the yield point. However, Kanai reported that the stretching force at a later stage changes with the amount of the component with a long relaxation times measured by melt viscoelasticity. It is known that high molecular weight components cause long relaxation times, but the flow-ability falls only if the amount of high molecular weight components is increased. In order to maintain the flow-ability in the case of increasing of the high molecular weight components, widening the molecular weight distribution is considered to be a good method of controlling the stretching force at a later stage.

However, there is no research showing the relationship between the stretching force obtained by table tenter and the actual thickness uniformity data obtained by a sequential and biaxially oriented stretching machine. It is suspected that uneven thickness of the film is the cause of film breaking during the stretching process and this is also believed to be one of the reasons making thinner films difficult. Therefore, film thickness uniformity is considered to be an important barometer of stretchability. This report will show the prediction of stretchability using a table tenter and the test results of film thickness uniformity using a sequential and biaxially oriented stretching machine.

Experiments

Samples

All samples were polymerized by Ziegler-Natta catalyst with different donors in order to change the molecular structure of isotacticity and molecular weight distribution. Sample A which is generally used for BOPP film produced commercially in our company as a grade name of F-300SP was used as a standard sample. Sample V with high isotacticity produced our middle size of our pilot plant was prepared in order to investigate the relationship between stretchability and crystallinity. Then three samples with low crystallinity from B1 through B3, and two wide molecular weight distribution samples C1 and C2 were prepared by our pilot plant in order to investigate the relationship between stretchability and resin properties (Table 1, Fig.3). To decrease the crystallinity, B1 and B2 were copolymerized with small amount of ethylene, and the isotacticity parameter meso pentad values mmmm measured by Carbon-13 Nuclear Magnetic Resonance (^{13}C -NMR) Spectroscopy [19] of B3 was reduced. The molecular weight distribution parameter M_w/M_n measured by gel permeation chromatography (GPC) of B1 and B2 were narrower than that of the standard sample A. M_w/M_n of C1 and C2 were larger than that of the standard sample A with the same isotacticity. Heptanes insolubilities (C7-II) measured by soxhlet abstraction method were used to compare with the crystallinity of each sample. Thermal properties of Melting point (T_m), melting enthalpy (ΔH_m), and crystallizing temperature (T_c) were measured by differential scanning

calorimetry (DSC). These seven samples with different properties in crystallinity and molecular weight distribution were used to investigate the relationship with the stretchability.

Stretching test using a table tenter

A non-stretching sheet, with a thickness and width of 1mm and 270mm respectively, was made by a sheet forming machine (Tanabe Plastics Co., Ltd) at a chilling roll temperature of 30°C. The sheet was stretched 4.6 times in the machine direction at 147°C which all samples was stretched properly by a heated roll type stretching machine (Iwamoto Seisaku-sho Co., Ltd).

Uniaxially stretched sheet in the machine direction was cut to the size of 290mm in length (machine direction) and 82mm in width (transverse direction), and was stretched in a transverse direction by the table tenter (Iwamoto Seisaku-sho Co., Ltd). The stretching ratio was 9.2 at several temperatures after preheating for 1 minute. At last a BOPP film with a thickness of 24μm was obtained. The stretching force was measured by a load cell which was equipped on a chuck of the table tenter to predict the stretchability of each sample.

The force data was determined as follows. A stress-strain curve of PP is shown in Fig.4. It was defined that the local maximum force observed at the beginning of the strain as the stretching force at the yield point (F_y), the minimum drawing force observed in the middle of the strain as the minimum drawing stretching force (F_d), and the stretching force observed at the end of the strain as the stretching force at the maximum strain (F_m) respectively. The stretching ratio at F_d was defined as the R_d . These stretching force parameters were used to predict stretchability. The film thickness uniformity of PP- α was predicted to be good, because its F_m is bigger than F_y , that is to say the stretched part gets harder than the non-stretched part. The stretched part requires more effort to be stretched than the non-stretched part. The resin design which indicates the PP- α 's stress-strain curve, such as low F_y and high F_m is believed to be necessary in order to improve the stretchability. Therefore F_m/F_y is considered to be one of the parameters of stretchability. It is believed that PP resin with more than one F_m/F_y should have good stretchability and PP resin with less than one F_m/F_y should have poor stretchability. The investigation on stretchability from the point of F_m/F_d is reported in this paper.

Stretching test using a sequential and biaxially oriented stretching machine

BOPP films were produced by a sequential and biaxially oriented stretching machine (Mitsubishi Heavy Industries Co., Ltd) using samples from B1 to C2 and the standard sample A. PP resins were extruded by an HM tandem type extruder with a discharge amount of 390kg/hr, and a non-stretched sheet with width of 270mm width was made using a roll type casting machine at the roll temperature of 30°C, and take-off speed of 55m/min. After

the sheet was stretched in a machine direction for 4.5 times at 138°C using heated rolls, BOPP film of 15µm thickness and 1m width was obtained through a tenter process with a stretching ratio to the transverse direction 9.5 times. Final machine speed was 270m/min and the strain rate was 423%/s which is close to that of a large size production line of BOPP film. The stretchability of each sample was verified by judging a thickness uniformity which is considered to be one of the important barometers of stretchability of BOPP film which was measured by film thickness distribution.

Results and Discussion

Examination for predicting a stretchability using a table tenter

At first, the influence of crystallinity on stretchability was examined with samples A and V which have quite different meso pentad values mmmm as parameters of crystallinity (Table 2, Fig.5). F_y value of sample V with mmmm value 97mol% at 164°C and 166°C indicated 2.49kgf and 1.90kgf respectively. They were 2.5 times as high as those of the standard sample A with mmmm value 90mol%. Stretching force at the yield point increased with increases of the sample's crystallinity, but the estimation was made that the difference of crystallinity will be about 6°C, that is to say, stretching force at the yield point of sample V will be equal to that of sample A if the stretching temperature of sample V was raised by 6°C. However, F_m values of sample V at 164°C and 166°C were 1.9 and 2.0 times as high as those of sample A at the same temperature. The ratios of F_m/F_d values of sample V were smaller than those of sample A, because the molecular weight distribution M_w/M_n of sample V (4.2) was smaller than that of sample A (4.5).

The sheet made by low crystallinity PP sample A was stretched without breaking at the stretching temperature between 158°C and 166°C, meaning sample A had a process window of 8°C. However, even though the sheet made by high crystallinity sample V (97%) was successfully stretched from 166°C to 172°C, it broke during stretching at 164°C. It was found that the stretchability of sample V was inferior to that of sample A, because the process window of sample V was 6°C, which means it is 2°C narrower than that of sample A. A possible reason is the influence of the narrower composition distribution of sample V, compared to sample A (Fig.6, Table 3). It means that the difference in temperature between the molten part of 70wt% and that of 40wt% of sample V (5.9°C), which is related to the process window of stretchability, is narrower than that of sample A (7.7°C). Since a proper amount of molten part is necessary to stretch for BOPP film as was studied by Uehara in double bubble tubular stretching process [20-23], widening the composition distribution is an effective method in improving its processability in tenting stretching process.

The stretching forces F_y , F_d , and F_m obtained from these stretching curves were plotted in Fig.7 (a). F_y

and F_d of sample V indicated almost the same value as those of sample A when its temperature was lowered by 6°C , but F_m of sample V was lower than that of sample A as the stretching temperature was lowered. The stretching force ratio F_m/F_y and F_m/F_d calculated from each stretching force are plotted in Fig. 7 (b). Since both F_m/F_y values of sample A and V increased with increasing of stretching temperature, stretchability was considered to be better at higher temperature in this range. However, since F_m/F_y of sample V at the range of 164 to 170°C were less than 1.0, it would only enable us to produce BOPP film of sample V with poor film thickness uniformity even if the film breaking did not occur. In other words, sample V is required to be stretched at only from 170°C to 172°C to make BOPP film with a good thickness uniformity. Therefore, sample V has quite a narrow process window in terms of film quality even though it has a process window of 6°C from 164°C to 170°C .

In the mean time, both F_m/F_d values of sample A and V decreased gradually with increasing the temperature. As F_d is a value that depends on average molecular weight and crystallinity, it is estimated that F_m/F_d is related to the amount of high molecular weight component to the average of molecular weight for the same crystallinity samples. F_m/F_d of sample V was lower than that of sample A, because the molecular weight distribution of sample V was narrower than that of sample A. F_m/F_d should decrease as the temperature rises, because the force of entanglement reduces as the temperature rises.

It was found that the stretching ratio R_d at the lowest stretching force of sample V was larger than that of sample A (Table 2, Fig.5). The stretching ratio of sample V must be higher than that of sample A in order to alter the crystallinity component. Therefore, stretchability of sample A is assumed to be better than that of sample V at the same temperature, even when the temperature was raised by 6°C to fit the stretching force at the yield point.

Further research for the purpose of grasping the relationship between the stretchability and resin properties was conducted using 6 samples from B1 to C2 and the standard sample A. The stretching force curve at 164°C obtained by table tenter is indicated in Fig.8. The stretching forces F_y at the yield point of samples from B1 to B3 with reduced crystallinity were lower than that of the standard sample A (Fig.8 (a)). The stretching forces F_m observed at the maximum stretching ratio of samples C1 and C2 were larger than that of sample A. The effect of wide molecular weight distribution was confirmed (Fig.8 (b)). The stretching force data at 164°C is indicated on Table 4.

The stretchability of each sample was predicted by connecting the stretching force parameter with molecular weight distribution M_w/M_n (Fig.9). As a result, it was predicted that the stretchability of all samples except for B1 is assumed to be greater than that of the standard sample A, because F_m/F_y of all the samples except for B1 were higher than that of A (Fig.9 (a)). Also, F_m/F_y was determined as the parameter related to both crystallinity and molecular weight distribution, because the data was able to fit into two lines with the same range

of C7-II (heptanes' insolubilities) which was one of the parameters of crystallinity. It was assumed that the stretchability improved with an increase of Mw/Mn and a decrease of crystallinity from Fm/Fy parameter. The stretchability of low crystallinity sample B1 did not improve compared to sample A, because the effect to worsen the stretchability by narrow Mw/Mn was greater than the effect to improve the stretchability by low crystallinity more effective.

However, it was recognized that the Fm/Fd is a parameter in proportion to Mw/Mn (Fig.9 (b)). The amount of the long time relaxation component becomes larger when the molecular weight distribution is widened which causes strain hardening. It is important to select a suitable extruder in order to maintain its long time relaxation component, because PP molecular weight distribution is easily shortened by degradation under severe conditions in the extrusion process [24].

Examination for verifying stretchability using a sequential and biaxially oriented stretching machine

Next, an experiment was conducted to verify stretchability of each sample by measuring film thickness uniformity using a sequential and biaxially oriented stretching machine. BOPP film thickness distribution was controlled by checking its thickness with a β -ray thickness gauge during production, and reflected the data to die clearance distribution (Fig.1) [25]. The film thickness uniformity data was measured after its distribution was roughly stabilized.

The film rolled on a winder was cut, and thickness τ for 2000 points to the transverse direction and 10 points to the machine direction were measured. The film thickness uniformity was evaluated to the transverse direction using the standard deviation σ calculated by equation (1).

$$\sigma = \frac{1}{2000} \sqrt{\sum_{n=1}^{2000} (\tau_n - \tau_{ave})^2} \quad \text{--- (1)}$$

Where τ_n is film thickness and τ_{ave} is average of film thickness.

But it was uncertain if σ was suitable for estimating the thickness uniformity, because we were unable to decide if σ was the best data for each sample due to the shortage of experiment time and sample amount. Furthermore, it was probable that the thickness distribution in the transverse direction was different even if the lip clearance was the same because each sample has its own flow feature. Therefore, film thickness variation coefficient in the machine direction δ calculated by equation (2) was used, which enable to estimate the amount of difference between the film thickness at the same point to the transverse direction. Since δ is most unlikely to be

influenced by experiment time or sample amount, even if film thickness distribution in the transverse direction is not good, δ can tell us the film thickness uniformity. Consequently, we came to the conclusion that the film thickness variation coefficient in the machine direction δ is the most important barometer to evaluate the stretchability of each sample.

$$\delta = \frac{1}{2000} \sum_{j=1}^{2000} \sqrt{\frac{1}{9} \sum_{i=1}^9 (\tau_{i,j} - \tau_{i+1,j})^2} \quad \text{--- (2)}$$

Where τ is film thickness, subscript i is the i -th point to the machine direction, and subscript j is the j -th point to the transverse direction.

Before checking the film thickness, the stretching behavior on the machine direction stretching roll was observed. It could be seen from the result of all samples tests, vibrations of the stretching line on the stretching roll occurred for B1 and B2. The stickiness of B1 and B2 to the roll is assumed to be much higher than that of other samples, because the accumulated weight ratio of melting parts of B1 and B2 at the roll temperature of 138°C is larger than that of other samples (Fig.10, Table 5). Vibration occurred when the balance between the stickiness of resin to the roll and the stretching force was changed. Meanwhile, the narrower molecular weight distribution of B1 and B2 is considered to be one of the causes of the vibrations (Fig.11). Since it is a well known fact that the phenomenon known as neck-in of the sheet easily occurs for resins with a narrow molecular weight distribution due to the lack of melt tension, the thickness of the edge should be thicker than average (namely edge beads and the edge part easily detach from the stretching roll). Therefore, it is considered that the stretching line of B1 and B2 are not as stable as other samples.

Next, film thickness variation coefficients in the machine direction δ and the standard deviation to the transverse direction σ were checked. Both of δ and σ showed a good correlation with the stretching force ratio F_m/F_y obtained by the table tenter (Table 6, Fig.12). The film thickness uniformity of all samples except for B1 improved in comparison to the standard sample A as was predicted by the table tenter. But the film thickness uniformity of lower crystallinity sample B3 obtained by a sequential and biaxially oriented stretching machine was not as good as was expected. It is supposed that F_y of sample B3 obtained by the table tenter is assumed to be smaller than we estimated, because the stretching temperature of the sequential and biaxially oriented stretching machine was 160°C, while the table tenter was at 164°C. On the other hand, F_m/F_d is also a good parameter to predict δ and σ (Fig.13). Low crystallinity sample B3 had a good correlation with other samples, because F_m/F_d is a parameter related to the molecular weight distribution.

Finally, the relationship between the resin parameter and stretchability is indicated in Fig.14. It is

thought to be a good method to widen molecular weight distribution to improve the film thickness uniformity parameters δ and σ . Even though sample A has a wider molecular weight distribution than sample B1, its σ and δ were almost identical to that of sample B1. Sample A should have been stretched at a higher temperature than sample B1 because the melting point of sample A is higher than that of sample B1. But two samples were stretched at the same temperature, δ and σ value of sample A did not meet the expected values. Therefore it was concluded that reducing the crystallinity and widening the molecular weight distribution is a good method to make a film with proper thickness uniformity.

Conclusion

Stretching force parameters obtained by a table tenter were investigated in order to predict the stretchability, to develop new materials to satisfy the demands of higher production speeds and thinner films. After the analysis on F_m/F_y and F_m/F_d was conducted, it was predicted that the stretchability of PP resin will improve by widening the molecular weight distribution and reducing the crystallinity. It was also found that reducing the crystallinity is effective in widening the process window of the stretching temperature in the stretching process.

By means of the test using a sequential and biaxially oriented stretching machine, reducing the crystallinity of PP resin by copolymerization was found not to be a good method in order to improve the stretchability, because the vibrations of the stretching line on the MD rolls occurred and made the film thickness unstable. It was verified that the film thickness uniformity which was the barometer of stretchability obtained from a sequential and biaxially oriented stretching machine gave a good correlation with F_m/F_y and especially F_m/F_d . That is to say, reducing the crystallinity of PP resin and widening the molecular weight distribution were effective in improving the film thickness uniformity. It is supposed that bad film thickness uniformity is the cause of film breaking. Therefore, it is important to improve the film thickness uniformity to produce BOPP films at higher rate and to make thinner films.

It was concluded that film thickness uniformity obtained by sequential and biaxially oriented stretching machine had a good relationship with the stretching force parameter obtained by a table tenter. Finally, the analysis of the stretching force obtained by a table tenter with a small amount of resin was an effective technique in predicting the stretchability of BOPP film.

References

1. *Kagaku-Keizai*, **3**, 88(2009)
2. J. E. Spruiel, J. L. White, *Polym. Eng. Sci.*, **15**, 550 (1975)
3. H. P. Nadella, H. M. Henson, J. E. Spruiel, J. L. White, *J. Appl. Polym. Sci.*, **27**, 3003 (1977)
4. H. P. Nadella, J. E. Spruiel, J. L. White, *J. Appl. Polym. Sci.*, **22**, 3121 (1978)
5. Y. Shimomura, J. L. White, *J. Appl. Polym. Sci.*, **27**, 2663 (1982)
6. J. L. White, *Film Processing*, Hanser Publishers., 412 (1990)
7. V. Rauschenberger, *ANTEC Proceeding*, 152 (1998)
8. Y. Koike, and M. Cakmak, *Polymer*, **44**, 4249 (2003)
9. R. A. Phillips, T. Nguyen, *J. Appl. Polym. Sci.*, **80**, 2400 (2001)
10. T. Kanai, F. Yonekawa, and I. Kuramoto, *17th Polym. Proc. Society Annual Meeting Abstracts*, 17 (2001)
11. T. Kanai, *Seikei-Kakou*, **18**(1), 53 (2006)
12. T. Kanai, N. Matsuzawa, T. Takebe, T. Yamada, *Polymer Processing Society Regional Meeting Europe CD-ROM Abstracts* (2007)
13. T. Kanai, N. Matsuzawa, H. Yamaguchi, T. Takebe, T. Yamada, *Europe Regional Polymer Processing Society Annual Meeting CD-ROM Abstracts* (2007)
14. T. Kanai, *24th Polymer Processing Society Annual Meeting CD-ROM Abstracts* (2008)
15. K. Iwakura, Y. D. Qang, M. Cakmak, *Int. Polym. Process.*, **7**, 327 (1992)
16. M. Cakmak, M. Simhambhatla, *Polym. Eng. Sci.*, **35**, 1562 (1995)
17. M. F. Butler, A. M. Donald, A. J. Ryan, *A. Polym.*, **39**, 39 (1998)
18. R. A. Phillips, G. Hebert, J. News, M. Wolkowicz, *Polym. Eng. Sci.*, **34**, 1731 (1994)
19. A. Zambelli, P. Locatelli, G. Bajo, A. Bovey, *Macromolecules*. **8**, 687 (1975)
20. H. Uehara, K. Sakauchi, T. Kanai, T. Yamada, *Int. Polym. Process.*, **19**(2), 155 (2004)
21. H. Uehara, K. Sakauchi, T. Kanai, T. Yamada, *Int. Polym. Process.*, **19**(2), 163 (2004)
22. H. Uehara, K. Sakauchi, T. Kanai, T. Yamada, *Int. Polym. Process.*, **19**(2), 172 (2004)
23. T. Kanai, H. Uehara, K. Sakauchi, T. Yamada, *Int. Polym. Process.*, **5**, 449 (2006)
24. H. Kometani, T. Matsumura, T. Suga, T. Kanai, *Int. Polym. Process.*, **21**(1), 24 (2006)
25. Y. Otomi, K. Kawasaki, JP-A-58-39050 (1983)

- Fig.1 Schematic diagram of BOPP film sequential and biaxially oriented stretching machine
- Fig.2 Relationship between thickness uniformity of BOPP film and the strain-stretching force curve
- Fig.3 DSC charts ((a), (c) and (e)) and GPC charts ((b), (d) and (f)) of each sample
- Fig.4 The definition of stretching parameters of F_y , F_d , R_d and F_m
- Fig.5 Stress -strain curve of (a) sample A and (b) sample V at several stretching temperatures
- Fig.6 Accumulated weight ratio of the molten part on DSC of each sample measured by DSC
- Fig.7 (a) Stretching force and (b) stretching force ratio of sample A and V
- Fig.8 Strain-Stress curve of (a)low crystallinity samples and (b)wide MWD samples
- Fig.9 Relationship between M_w/M_n and (a) F_m/F_y , (b) F_m/F_d
- Fig.10 Accumulated weight ratio of the melting parts on DSC (wt%)
- Fig.11 Sheet Vibration on the MD stretching roll
- Fig.12 Relationship between F_m/F_y and film thickness uniformity parameter (a) δ , (b) σ
- Fig.13 Relationship between F_m/F_d and film thickness uniformity parameter (a) δ , (b) σ
- Fig.14 Relationship between M_w/M_n and film thickness uniformity parameter (a) δ , (b) σ
 (The number in the parentheses is C7-II of each sample.)

Table 1 Resin properties of samples

Table 2 Stretching parameters of sample A and V obtained by a table tenter

Table 3 Accumulated weight ratio of the molten part of each sample measured by DSC

Table 4 Stretching parameters of sample from A to C2 obtained by a table tenter

Table 5 Sheet Vibration on the MD stretching roll (○:not occurred ×:occurred)

Table 6 Film thickness uniformity parameter δ and σ obtained by a sequential and biaxially oriented stretching machine

Table 1 Resin properties of samples

Properties	Unit	Standard	High crystallinity	Low crystallinity			Wide MWD	
		A	V	B1	B2	B3	C1	C2
MFR	g/10min	3.0	3.0	3.0	3.1	2.9	2.7	3.2
mmmm	mol%	90	97	-	-	88	90	90
C2 ⁼ amount	wt%	0.0	0.0	0.5	0.4	0.0	0.0	0.0
C7-II	wt%	96.7	99.0	97.4	97.3	95.9	93.9	94.7
Tm	°C	161.4	165.7	159.7	158.4	160.4	162.0	162.4
ΔHm	J/g	99.6	111.0	99.4	100.2	97.3	98.2	98.3
Tc	°C	102.0	105.4	103.0	102.8	101.7	101.7	104.1
Mw(× 10 ⁻⁵)	-	3.56	3.61	3.29	3.50	3.60	3.81	3.69
Mn(× 10 ⁻⁴)	-	7.73	8.68	9.14	8.53	7.79	7.00	6.63
Mw/Mn	-	4.6	4.2	3.6	4.1	4.6	5.4	5.6

Table 2 Stretching parameters of sample A and V obtained by a table tenter

Stretching parameters	Sample	Stretching temperature (°C)							
		158	160	162	164	166	168	170	172
Fy (kgf)	A	2.51	1.85	1.55	1.00	0.74	-	-	-
	V	-	-	-	2.49	1.90	1.38	0.94	0.59
Fd (kgf)	A	1.83	1.30	1.15	0.73	0.65	-	-	-
	V	-	-	-	1.85	1.19	0.99	0.77	0.49
Rd (-)	A	3.9	5.0	4.8	5.5	5.1	-	-	-
	V	-	-	-	8.2	6.1	6.2	6.5	6.5
Fm (kgf)	A	2.40	1.89	1.58	1.03	0.83	-	-	-
	V	-	-	-	1.92	1.62	1.23	0.93	0.61
Fy/Fd (-)	A	1.37	1.42	1.35	1.37	1.14	-	-	-
	V	-	-	-	1.35	1.60	1.39	1.22	1.20
Fm/Fd (-)	A	1.31	1.45	1.37	1.41	1.28	-	-	-
	V	-	-	-	1.04	1.36	1.24	1.21	1.24
Fm/Fy (-)	A	0.96	1.02	1.02	1.03	1.12	-	-	-
	V	-	-	-	0.77	0.85	0.89	0.99	1.03

Fy: Stretching force at yield point, Fd: Minimum stretching force at drawing,

Rd: Stretching ratio at minimum stretching force, Fm: Stretching force at maximum ratio

Table 3 Accumulated weight ratio of the molten part of each sample measured by DSC

Accumulated weight ratio of molten part (wt %)	Temperature (°C)	
	A	V
10	117.6	127.4
30	146.8	154.2
40	152.7	158.9
50	156.2	161.7
60	158.6	163.4
70	160.4	164.8
90	163.9	167.6

Table 4 Stretching parameters of sample from A to C2 obtained by a table tenter

Samples	Stretching Parameters						
	Fy (kgf)	Fd (kgf)	Rd (-)	Fm (kgf)	Fy/Fd (-)	Fm/Fd (-)	Fm/Fy (-)
A	1.02	0.79	5.33	1.06	1.29	1.34	1.04
B1	0.97	0.75	6.0	0.98	1.29	1.31	1.01
B2	0.93	0.74	5.60	0.99	1.25	1.33	1.06
B3	0.92	0.77	4.8	1.05	1.19	1.36	1.14
C1	0.98	0.82	5.3	1.11	1.20	1.35	1.13
C2	0.94	0.79	5.3	1.10	1.19	1.39	1.17

Fy: Stretching force at yield point, Fd: Minimum stretching force at drawing,

Rd: Stretching ratio at minimum stretching force, Fm: Stretching force at maximum ratio

Table 5 Sheet Vibration on the MD stretching roll (○:not occurred ×:occurred)

Vibration	A	B1	B2	B3	C1	C2
Accumulated weight ratio of melting parts at 138°C on DSC (wt%)	21.1	23.4	24.2	21.5	19.6	18.7
Mw/Mn (-)	4.6	3.6	4.1	4.6	5.4	5.6
Sheet vibration	○	×	×	○	○	○

Table 6 Film thickness uniformity parameter δ and σ obtained by a sequential and biaxially oriented stretching machine

Film thickness uniformity	Samples					
	A	B1	B2	B3	C1	C2
δ (-)	0.62	0.63	0.50	0.48	0.39	0.35
σ (μm)	3.2	3.8	3.3	3.1	2.7	2.1

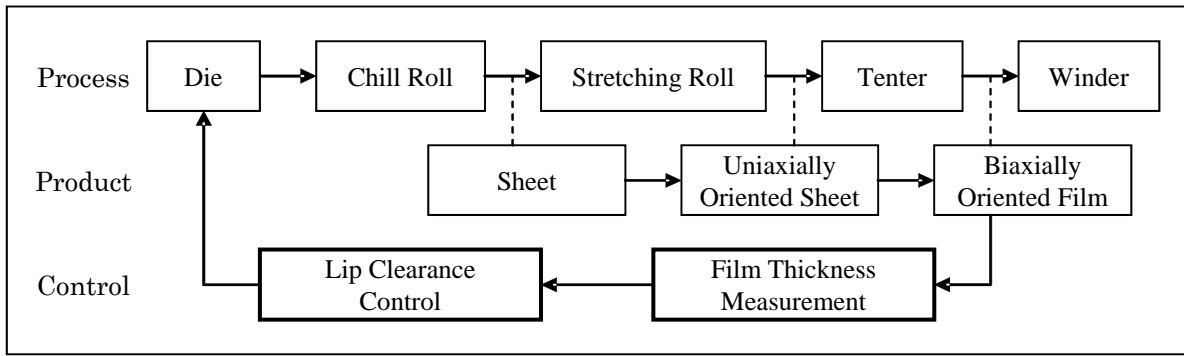


Fig.1 Schematic diagram of BOPP film sequential and biaxially oriented stretching machine

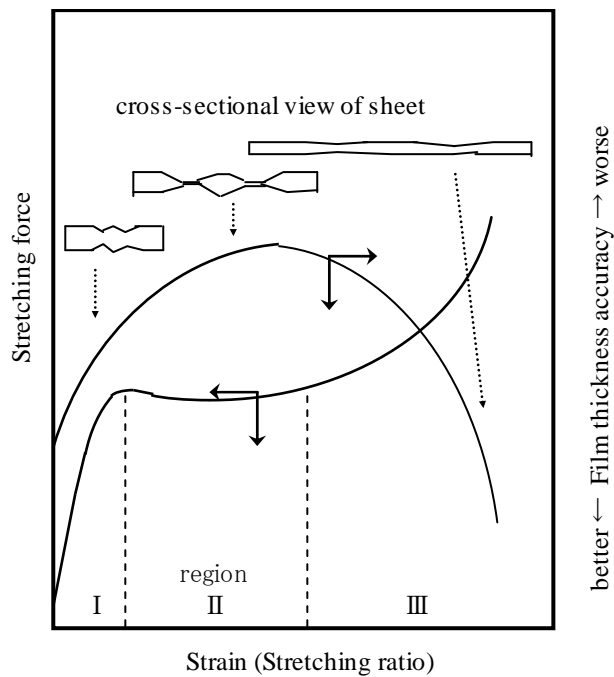


Fig.2 Relationship between thickness uniformity of BOPP film and the strain-stretching force curve

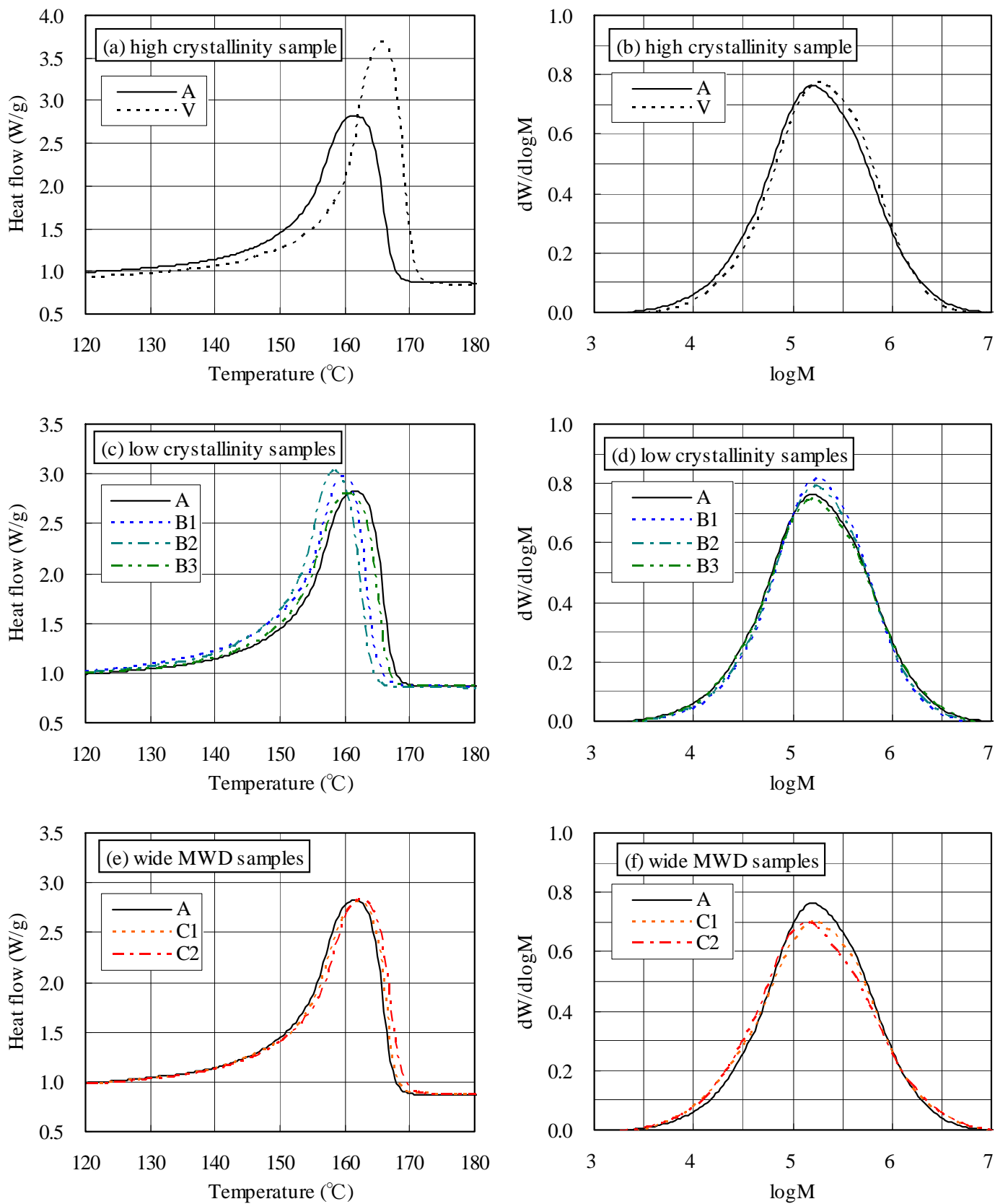


Fig.3 DSC charts ((a), (c) and (e)) and GPC charts ((b), (d) and (f)) of each sample

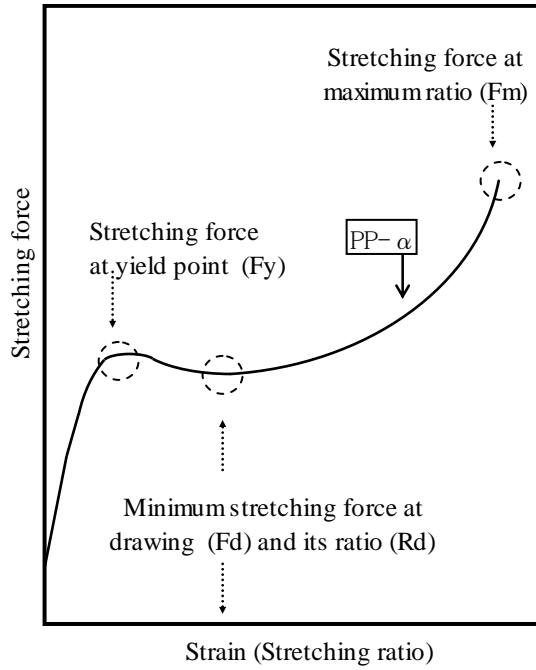


Fig.4 The definition of stretching parameters of F_y , F_d , R_d and F_m

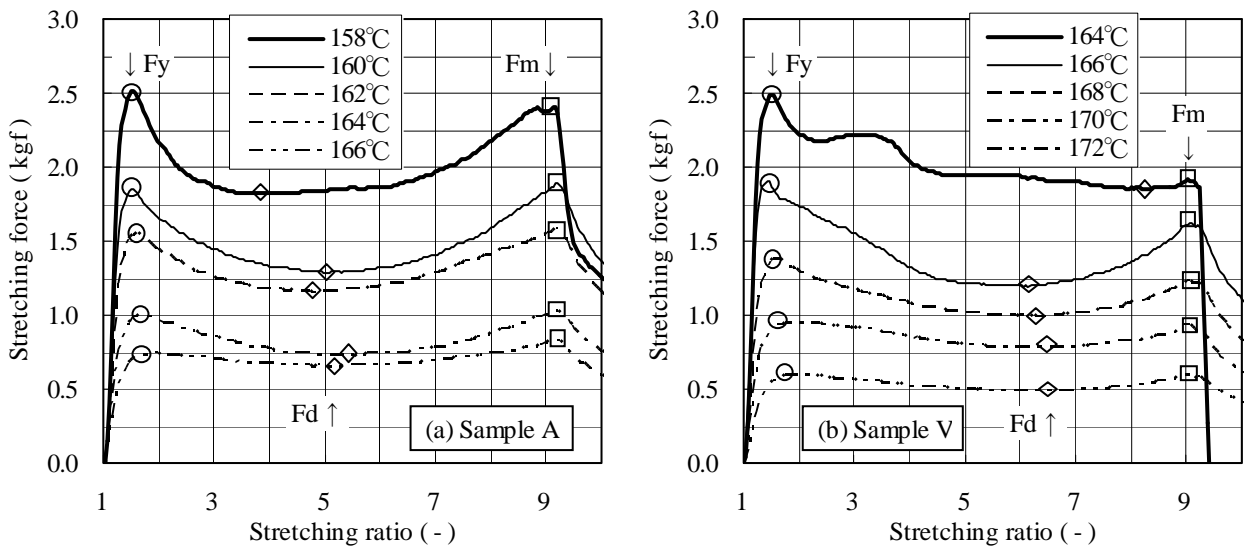


Fig.5 Stress -strain curve of (a) sample A and (b) sample V at several stretching temperatures

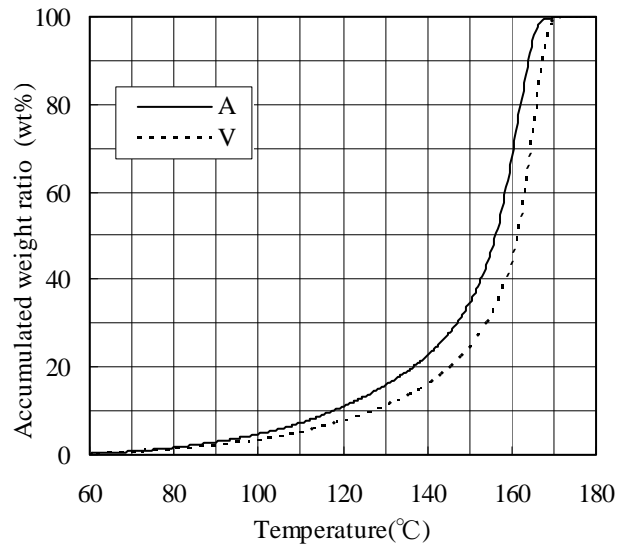


Fig.6 Accumulated weight ratio of the molten part on DSC of each sample measured by DSC

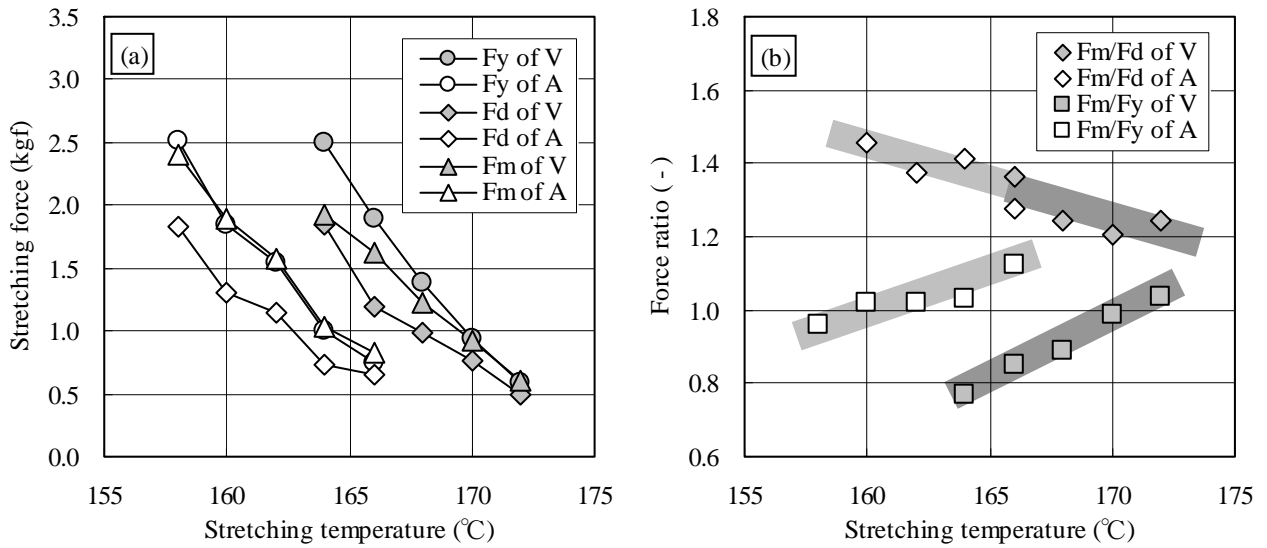


Fig.7 (a) Stretching force and (b) stretching force ratio of sample A and V

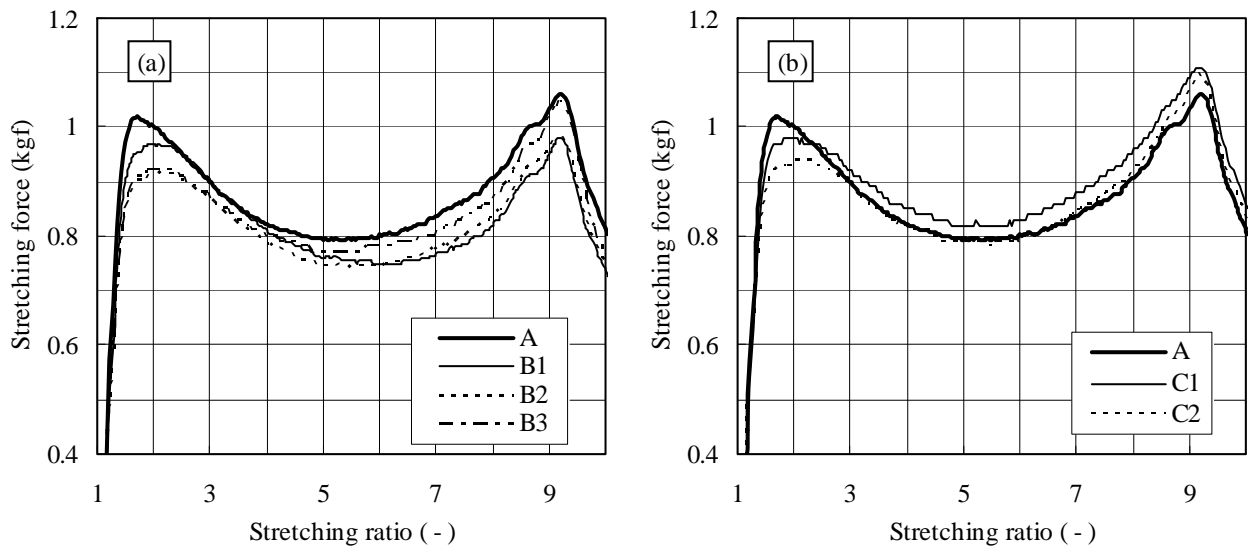


Fig.8 Strain-Stress curve of (a)low crystallinity samples and (b)wide MWD samples

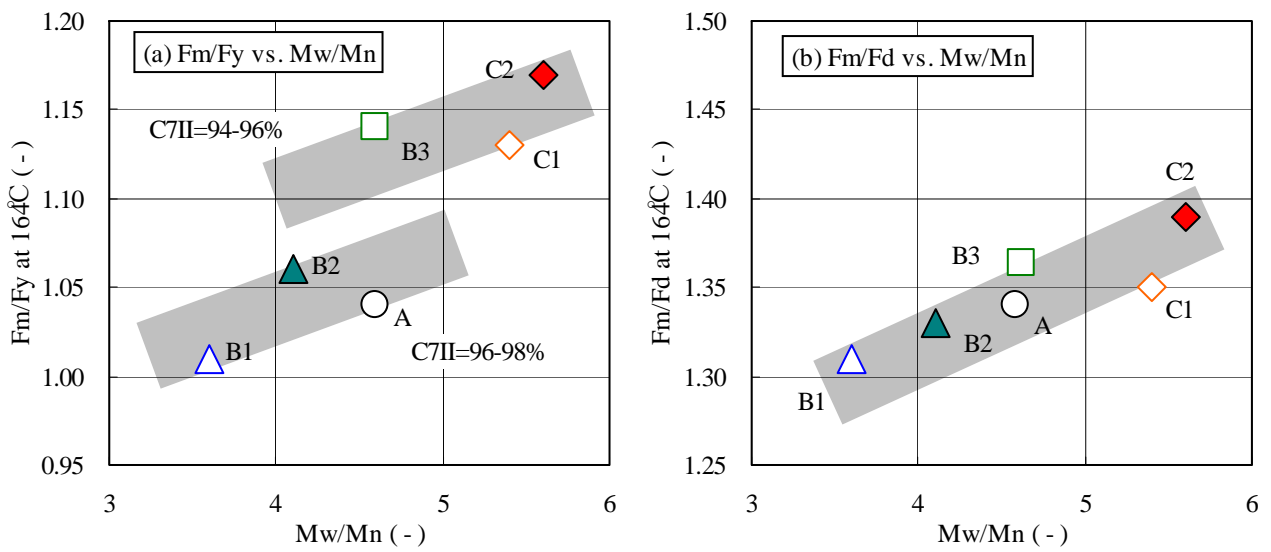


Fig.9 Relationship between Mw/Mn and (a)Fm/Fy, (b)Fm/Fd

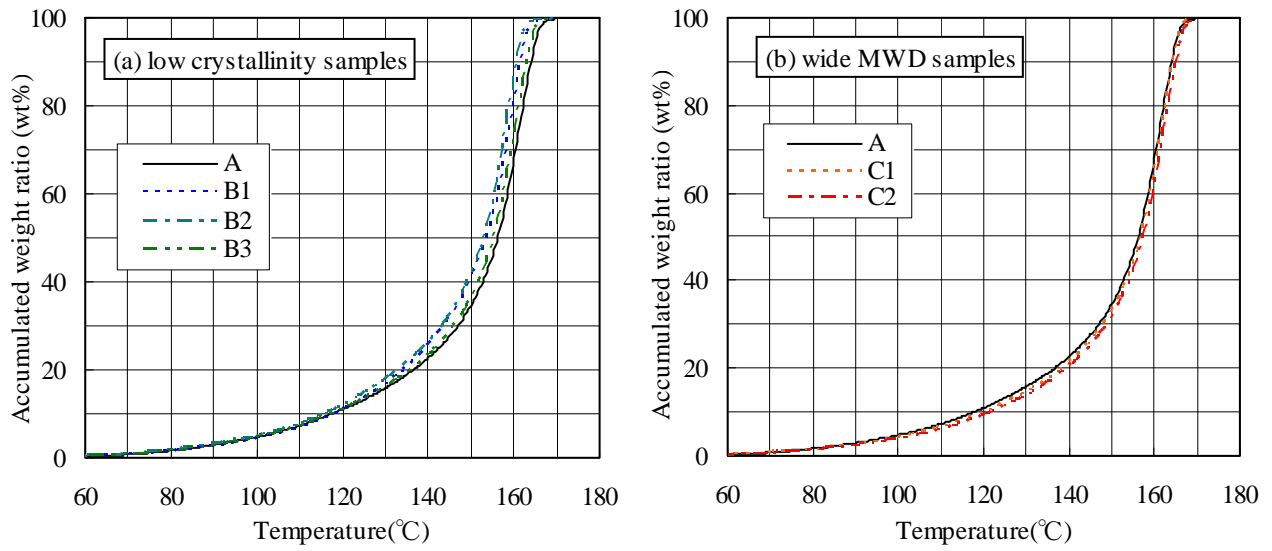


Fig.10 Accumulated weight ratio of the melting parts on DSC (wt%)

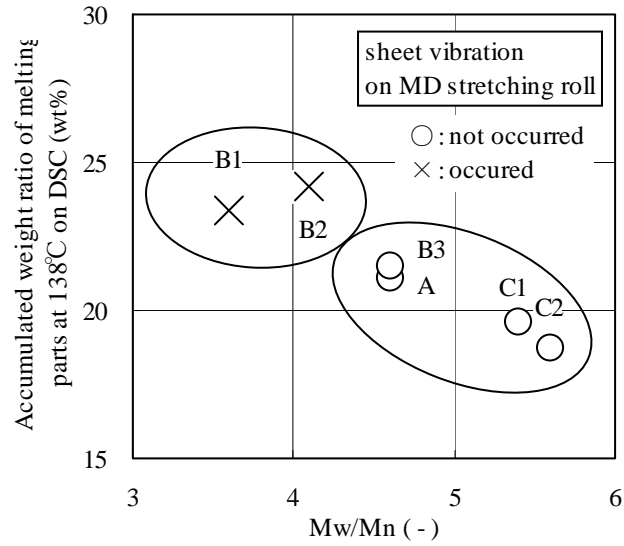


Fig.11 Sheet Vibration on the MD stretching roll

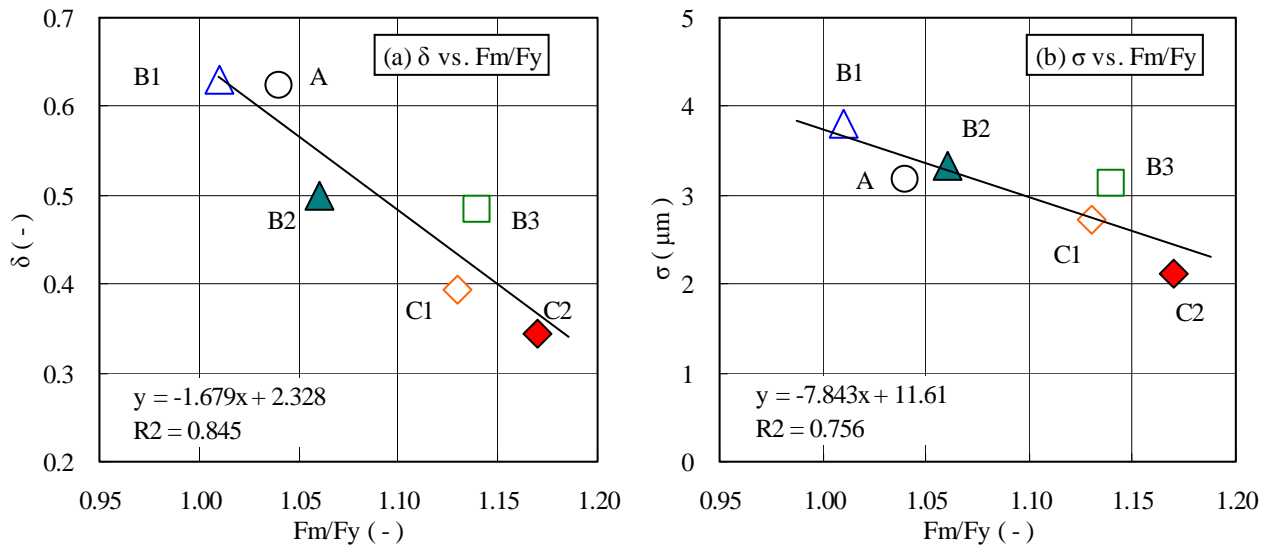


Fig.12 Relationship between Fm/Fy and film thickness uniformity parameter (a) δ , (b) σ

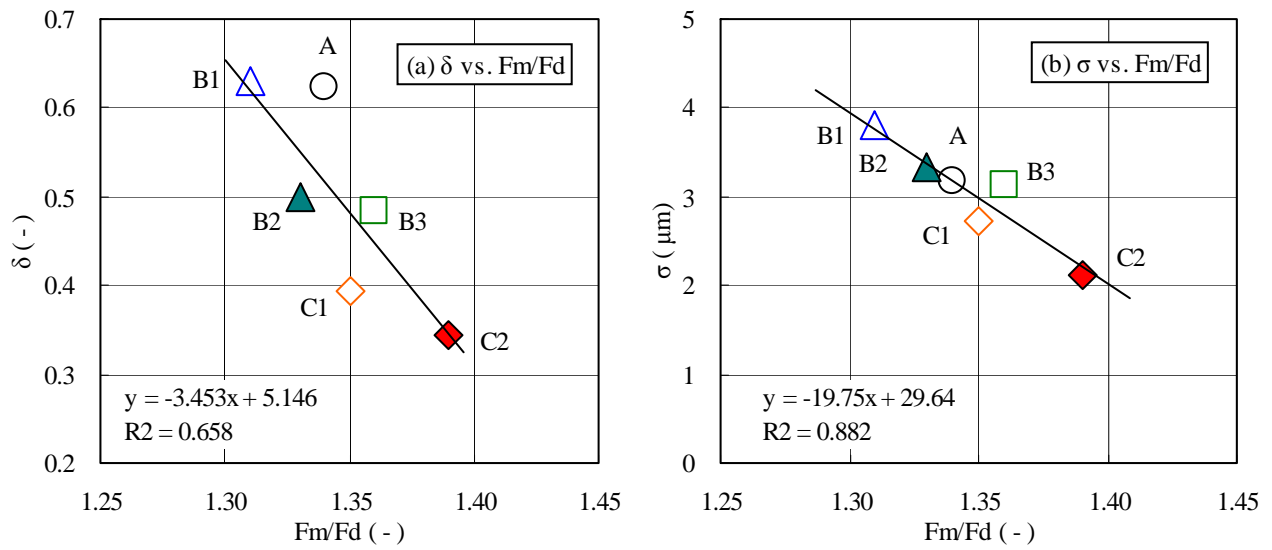


Fig.13 Relationship between Fm/Fd and film thickness uniformity parameter (a) δ , (b) σ

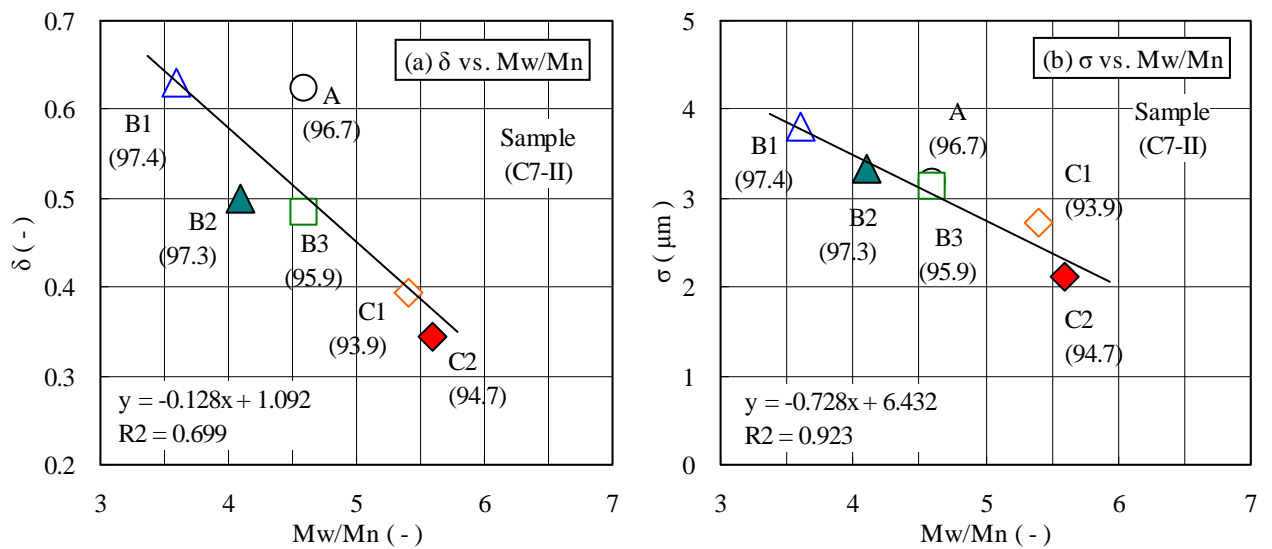


Fig.14 Relationship between Mw/Mn and film thickness uniformity parameter (a) δ , (b) σ
(The number in the parentheses is C7-II of each sample.)